



Cite this: *RSC Chem. Biol.*, 2022, 3, 848

Received 17th April 2022,  
Accepted 17th May 2022

DOI: 10.1039/d2cb00105e

rsc.li/rsc-chembio

## Rational design of a dual-reactive probe for imaging the biogenesis of both H<sub>2</sub>S and GSH from L-Cys rather than D-Cys in live cells†

Haishun Ye,<sup>a</sup> Longhui Cheng,<sup>id</sup> b Xiaoliang Tu,<sup>a</sup> Da-Wei Wang<sup>\*b</sup> and Long Yi<sup>id</sup> <sup>\*a</sup>

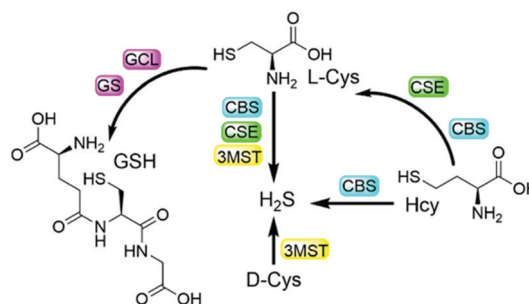
Biothiols and their interconversion are involved in cellular redox homeostasis as well as many physiological processes. Here, a dual-reactive dual-quenching fluorescent probe was rationally developed based on thiolysis reactions of 7-nitrobenzoxadiazole (NBD) tertiary amine and 7-cyanobenzoxadiazole (CBD) arylether for imaging of the biothiol interconversion. We demonstrate that the NBD-CBD probe exhibits very weak background fluorescence due to the dual-quenching effects, and can be dual-activated by H<sub>2</sub>S and GSH with an over 500-fold fluorescence increase at 525 nm. In addition, the probe shows high sensitivity, excellent selectivity, and good biocompatibility, all of which promote the simultaneous detection of both H<sub>2</sub>S and GSH in live cells. Importantly, probe 1 was successfully employed to reveal the biogenesis of both H<sub>2</sub>S and GSH from L-Cys rather than from D-Cys, and therefore, D-Cys would be solely converted into H<sub>2</sub>S, which may help understand the more H<sub>2</sub>S generation from D-Cys than from L-Cys in live cells.

## Introduction

Biothiols include small molecules of glutathione (GSH), cysteine (Cys), homocysteine (Hcy), and hydrogen sulfide (H<sub>2</sub>S), all of which play important roles in many physiological and pathological processes.<sup>1–7</sup> For example, biological H<sub>2</sub>S is considered to be a nitric oxide (NO)-like signaling molecule that is involved in the regulation of angiogenesis, vasodilation, metabolic bioenergetics, *etc.*<sup>2</sup> GSH is the most abundant biothiol in cells (1–10 mM), which majorly contributes to maintaining redox homeostasis and defending against toxins.<sup>3</sup> As shown in Scheme 1, endogenous H<sub>2</sub>S can be enzymatically produced from

Cys by cystathionine β-synthase (CBS), cystathionine γ-lyase (CSE), and 3-mercaptopyruvate sulfurtransferase (3MST)/cysteine aminotransferase (CAT),<sup>4a,b</sup> while GSH can be enzymatically generated from L-Cys by the consecutive actions of glutamate cysteine ligase (GCL) and GSH synthetase (GS).<sup>4c,d</sup> On the other hand, Hcy can be enzymatically transformed to generate cystathionine and then to Cys, as well as to H<sub>2</sub>S.<sup>4e</sup> Based on the metabolism and biotransformation of these pathways, the concentrations of biothiols are in dynamic equilibrium in live systems. In addition, abnormal levels of one or more different biothiols are closely related to many diseases including Alzheimer's disease, liver cirrhosis, renal/cardiovascular diseases, and cancers.<sup>5,6</sup> Moreover, protein post-translational modifications (PTMs) are also involved in interconversion of biothiols. For example, the S-glutathionylation of CBS under oxidative stress and GSH can promote the generation of endogenous H<sub>2</sub>S.<sup>7</sup> Therefore, the development of facile and reliable tools to study the interconversion and inherent crosstalk of these biothiols is of great value for related fundamental research.

Fluorescence-based methods are highly suitable and sensitive for *in situ* and real-time visualization of biomolecules. In the past decade, numerous fluorescent probes have been developed for the detection of biothiols in live systems.<sup>8</sup> In addition, probes with multiple reaction sites have been rationally designed for

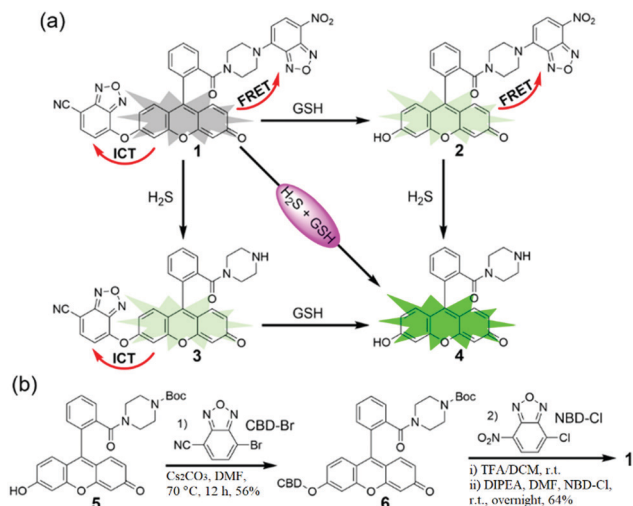


**Scheme 1** The metabolism and biotransformation pathways of different biothiols.

<sup>a</sup> State Key Laboratory of Organic-Inorganic Composites and Beijing Key Lab of Bioprocess, Beijing University of Chemical Technology (BUCT), Beijing 100029, China. E-mail: yilong@mail.buct.edu.cn

<sup>b</sup> State Key Laboratory of Elemento-Organic Chemistry and Department of Chemical Biology, College of Chemistry, National Pesticide Engineering Research Center, Nankai University, Tianjin, 300071, China. E-mail: wangdw@nankai.edu.cn

† Electronic supplementary information (ESI) available: Experimental details and additional figures. See DOI: <https://doi.org/10.1039/d2cb00105e>



**Scheme 2** (a) Schematic illustration of the design for a dual-quenching probe **1** based on the combination of NBD amine and CBD arylether, which can only be activated by both  $\text{H}_2\text{S}$  and GSH. FRET, fluorescence resonance energy transfer; ICT, intramolecular charge transfer. (b) Synthetic routine and conditions for probe **1**.

distinguishing different biothiols from each other with different emission channels.<sup>9</sup> It is noted that a strategy of using multi-reactive multi-quenching probes has been demonstrated to be useful for highly sensitive and selective detection of biothiols and other analytes.<sup>10,11</sup> Attachment of multi-reactive quenchers to the same fluorophore results in low-background fluorescence of the probe due to the multi-quenching fashions through multiplication effects,<sup>11</sup> which can be used to enhance the sensitivity and selectivity of the detection in complex biological environments. We as well as others further employed such a multi-quenching strategy to develop probes that require multiple activations from different analytes,<sup>12</sup> which can investigate the cooperative relationship of the analytes and differentiate cancer cells. Herein, we report the rational design and preparation of a dual-quenching probe for imaging the biogenesis of both  $\text{H}_2\text{S}$  and GSH from L-Cys rather than D-Cys in live cells.

As shown in Scheme 2, we combined the NBD and CBD moieties into a fluorescein to access the dual-quenching probe **1**. The thiolysis reactions of NBD amine<sup>10</sup> and CBD arylether<sup>13</sup> are specific sensing motifs for  $\text{H}_2\text{S}$  and GSH, respectively. The CBD moiety can quench the fluorescence through the intramolecular charge transfer (ICT) effect,<sup>13</sup> while the NBD amine moiety can switch off the fluorescence of the fluorescein through the fluorescence resonance energy transfer (FRET) effect.<sup>14</sup> As a result, probe **1** is highly quenched from the dual-quenching effects, and dual activations of this probe should result in significant fluorescence enhancement (Scheme 2a).

Probe **1** was prepared by a facile three-step synthesis from commercially available reagents (Scheme 2b). The coupling of fluorescein and boc-piperazine provided compound **5**, which was modified by CBD-Br to generate compound **6**. After deprotection of the boc group and further coupling with NBD-Cl, probe **1** was obtained in good yield. Structural identification was confirmed by  $^1\text{H}$  NMR,  $^{13}\text{C}$  NMR, and HRMS (see ESI†).

With the probe in hand, we investigated the absorbance spectra of probe **1** in the presence of  $\text{H}_2\text{S}$  and/or GSH in PBS buffer (50 mM, pH 7.4). The concentration-dependent absorbance of probe **1** in 0.5% DMSO-containing PBS suggested the good water solubility of the probe up to 80  $\mu\text{M}$  (Fig. S1, ESI†). After treatment with both  $\text{H}_2\text{S}$  (using  $\text{Na}_2\text{S}$  as an equivalent) and GSH, a sharp absorbance peak appeared at 500 nm, which is assigned to the fluorescein product **4** (Fig. S2a, ESI†). When  $\text{H}_2\text{S}$  alone was added, a new peak with low absorbance at 500 nm was also observed (Fig. S2b, ESI†), and there was an obvious overlap between the absorbance profile of NBD and the emission profile of **4** (Fig. S2c, ESI†), both of which support the existence of an intramolecular FRET effect in **2**. When **1** was treated by GSH alone, the absorption peak was obviously red-shifted from 470 nm to 500 nm, implying an ICT sensing mechanism (Fig. S2d, ESI†).

Probe **1** is essentially non-fluorescent ( $\Phi_1 = 0.18\%$ ) due to the FRET-ICT dual-quenching effects. After dual activations with  $\text{H}_2\text{S}$  (100  $\mu\text{M}$ ) and GSH (2 mM), the fluorescence of the probe increased significantly, with over 500-fold turn-on at 525 nm (Fig. 1a) and generating high bright **4** ( $\Phi_4 = 70.6\%$ ). When **1** was treated by  $\text{H}_2\text{S}$  or GSH alone, only slight fluorescence enhancements were observed (Fig. 1b and c), and the by-products NBD-SH and CBD-SG were non-fluorescent.<sup>80,13</sup> Time-dependent emissions at 525 nm suggested that probe **1** was stable in the absence of analytes and had obviously larger signal enhancement for  $\text{H}_2\text{S}$  + GSH than that of any single analyte (Fig. 1d). In addition, the data (Table S1, ESI†) suggest that the turn-on folds of the dual-reactive probe could be approximate multiplications of each turn-on fold of both single-reactive probes,<sup>11</sup> highlighting the advantage of the dual-reactive dual-quenching method.

To study the sensitivity of the dual-reactive probe, we incubated **1** with different levels of  $\text{H}_2\text{S}$  or GSH for 1 h in the

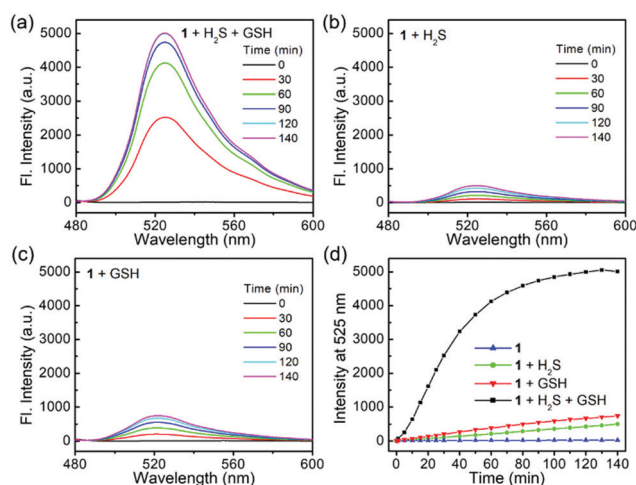


**Fig. 1** Time-dependent fluorescence responses of **1** (1  $\mu\text{M}$ ) toward  $\text{H}_2\text{S}$  (100  $\mu\text{M}$ ) and/or GSH (2 mM) in PBS buffer. (a) **1** was treated with  $\text{H}_2\text{S}$  and GSH, or only with  $\text{H}_2\text{S}$  (b) or GSH (c). (d) Time-dependent emissions at 525 nm for **1** treated with  $\text{H}_2\text{S}$  and GSH (black),  $\text{H}_2\text{S}$  (green), GSH (red) or probe alone (blue). Excitation, 469 nm.

presence of a certain concentration of another activator, after which the emission profiles were measured (Fig. 2). When probe **1** was treated with different concentrations of  $\text{H}_2\text{S}$  (0–100  $\mu\text{M}$ ) in the presence of GSH (2 mM), the emission at 525 nm was linearly enhanced to the concentrations of  $\text{H}_2\text{S}$  from 0 to 60  $\mu\text{M}$  (Fig. 2a and b). Similarly, when **1** was treated with various levels of GSH (0–10 mM) in the presence of  $\text{H}_2\text{S}$  (10  $\mu\text{M}$ ), we observed a fluorescence enhancement in a concentration-dependent fashion from 0–4 mM (Fig. 2c and d). Taken together, probe **1** can be used to detect the co-existence of  $\text{H}_2\text{S}$  and GSH.

One major requirement for a fluorescent probe is that it should exhibit a selective response toward the targeted analytes but not for other competing biological species. To this end, probe **1** was incubated with different reactive sulfur species ( $\text{SO}_3^{2-}$  and  $\text{S}_2\text{O}_3^{2-}$ ), other biothiols (Cys and Hcy) and reactive oxygen species ( $\text{H}_2\text{O}_2$  and  $\text{HOCl}$ ) in the presence of  $\text{H}_2\text{S}$  and/or GSH for 1 h. As shown in Fig. 3, the co-incubation of GSH or  $\text{H}_2\text{S}$  and small-molecules triggered a slight fluorescence increase. Therefore, probe **1** could be suitable for sensing the dual activations from  $\text{H}_2\text{S}$  and GSH in the presence of other biological analytes.

We also validated the sensing reactions of **1** by HRMS (Fig. S3, ESI†). Product **4** from the dual-activated reactions was observed as  $[\text{M} + \text{H}]^+$  401.1490 (calcd for  $\text{C}_{24}\text{H}_{21}\text{N}_2\text{O}_4^+$ , 401.1496). The  $\text{H}_2\text{S}$ -triggered product **3** and GSH-triggered product **2** were also observed as  $[\text{M} + \text{H}]^+$  544.1621 (calcd for  $\text{C}_{31}\text{H}_{22}\text{N}_5\text{O}_5^+$ , 544.1615) and  $[\text{M} + \text{H}]^+$  564.1513 (calcd for  $\text{C}_{30}\text{H}_{22}\text{N}_5\text{O}_7^+$ , 564.1514), respectively. We further used HPLC to monitor and validate the reaction mechanism (Fig. S4, ESI†). These results confirmed probe **1** for the dual-reactive detection of  $\text{H}_2\text{S}$  and GSH.

Encouraged by the above results, fluorescence imaging experiments were carried out to evaluate the potential of probe

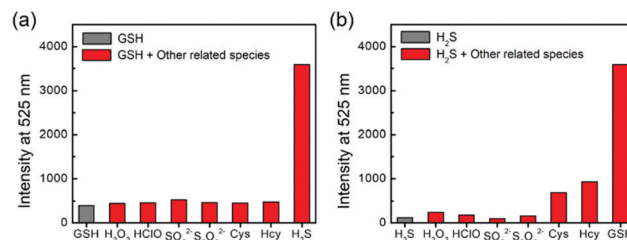


Fig. 3 (a) Emissions at 525 nm of **1** (1  $\mu\text{M}$ ) toward various biologically relevant species (100  $\mu\text{M}$ ) in the presence of GSH (5 mM). (b) Emissions at 525 nm of **1** (1  $\mu\text{M}$ ) toward 5 mM GSH and other various biologically relevant species (100  $\mu\text{M}$ ) in the presence of  $\text{H}_2\text{S}$  (100  $\mu\text{M}$ ). Excitation, 469 nm.

**1** for imaging in live HeLa cells (human cervical cancer cells). We first evaluated the cytotoxicity of **1** by the MTT assay. The results (Fig. S5, ESI†) suggested that probe **1** had a slight effect on cells after 24 h of incubation, and the cell viability at 50  $\mu\text{M}$  of probe **1** was still above 85%. HeLa cells contain nearly no endogenous  $\text{H}_2\text{S}$ <sup>15</sup> but a moderate level of endogenous GSH (5.4 mM).<sup>16</sup> As expected, HeLa cells treated with only probe **1** showed weak fluorescence, and when the cells were pre-incubated with 100  $\mu\text{M}$   $\text{Na}_2\text{S}$  and then with probe **1**, obvious green fluorescence was observed (Fig. 4). Therefore, the co-existence of intracellular  $\text{H}_2\text{S}$  and GSH can trigger the fluorescent turn-on response of probe **1**, which is consistent with the results in buffers.

In addition to the  $\text{H}_2\text{S}$  biosynthesis, L-Cys is also a substrate for GSH synthesis.<sup>4d</sup> D-Cys, which should be not a substrate for GSH due to the different chirality, can be metabolized to generate  $\text{H}_2\text{S}$ .<sup>4b</sup> On the other hand, our previous work indicated the imaging of more  $\text{H}_2\text{S}$  production from D-Cys than that from L-Cys.<sup>17</sup> We envisioned that metabolic differences of D-Cys and

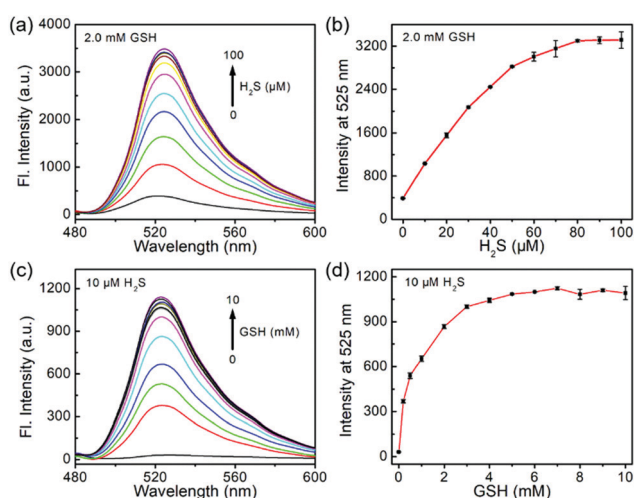


Fig. 2 (a) Fluorescence spectra and (b) emission at 525 nm of **1** (1  $\mu\text{M}$ ) toward different concentrations of  $\text{H}_2\text{S}$  in the presence of GSH (2 mM). (c) Fluorescence spectra and (d) emission at 525 nm of **1** (1  $\mu\text{M}$ ) toward different concentrations of GSH in the presence of  $\text{H}_2\text{S}$  (10  $\mu\text{M}$ ). Excitation, 469 nm.

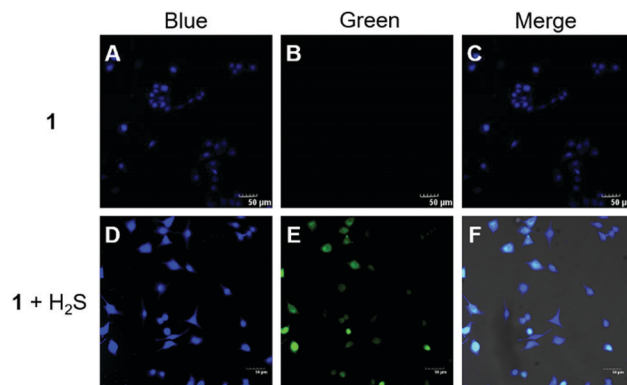
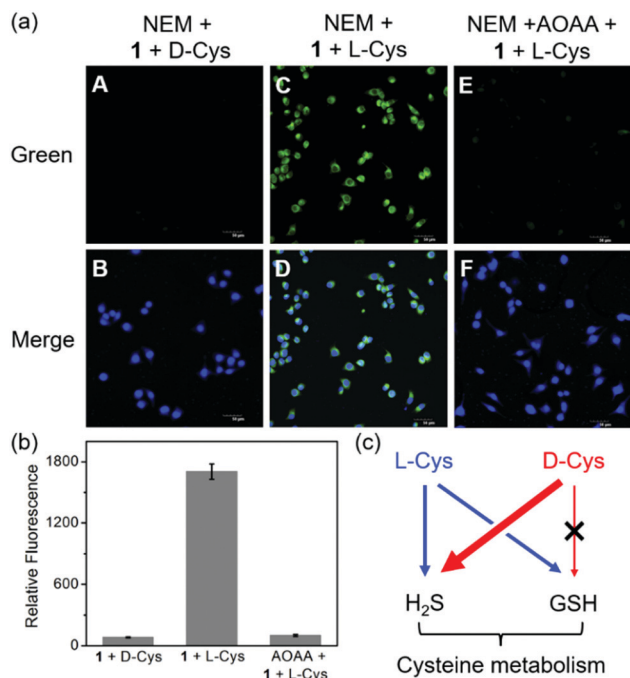


Fig. 4 Confocal microscopy images of HeLa cells with using probe **1** in the presence of endogenous GSH and exogenous  $\text{H}_2\text{S}$ . (A–C) Cells were only incubated with 10  $\mu\text{M}$  probe **1** for 60 min. (D and E) HeLa cells were pre-incubated with 100  $\mu\text{M}$   $\text{Na}_2\text{S}$  for 60 min, and then washed and incubated with 10  $\mu\text{M}$  probe **1** for another 60 min. After the incubation, the cells were treated with DAPI (2  $\mu\text{g mL}^{-1}$ ) for 10 min. (A and D) The blue fluorescence of DAPI (450–500 nm) with 405 nm excitation. (B and E) The green fluorescence of probe **1** (500–550 nm) with 488 nm excitation. (C and F) The merged images of blue and green fluorescence. Scale bar, 50  $\mu\text{m}$ .







**Fig. 5** Confocal microscopy images of HeLa cells after co-incubation with probe **1** and D-Cys or L-Cys. (a) After pre-treated with NEM (1 mM) for 30 min, (A and B) cells co-stimulated with 10  $\mu\text{M}$  probe **1** and 500  $\mu\text{M}$  D-Cys for 60 min; (C and D) cells co-stimulated with 10  $\mu\text{M}$  probe **1** and 500  $\mu\text{M}$  L-Cys for 60 min; (E and F) cells pre-incubated with AOAA (200  $\mu\text{M}$ ) for 30 min, then co-stimulated with 10  $\mu\text{M}$  probe **1** and 500  $\mu\text{M}$  L-Cys for 60 min. Then, the cells were incubated with DAPI (2  $\mu\text{g mL}^{-1}$ ) for 10 min. The merged images of the blue fluorescence of DAPI and green fluorescence of probe **1** are also indicated. Scale bar, 50  $\mu\text{m}$ . (b) Relative green fluorescence of images from (a),  $N = 3$  fields of cells, error bars are means  $\pm$  S.D. (c) Schematic representation of the chiral Cys metabolism in live cells.

L-Cys in live cells may be validated by our dual-reactive probe **1** from live-cell imaging. To this end, we removed the endogenous GSH by the thiol blocking reagent *N*-ethylmaleimide (NEM) of HeLa cells and then checked the intracellular fluorescence in the presence of chiral Cys using probe **1**. As shown in Fig. 5a, the green fluorescence was hardly detected in the D-Cys-treated cells, while strong fluorescence was observed in L-Cys-treated cells. In a control, we employed aminooxyacetic acid (AOAA, 200  $\mu\text{M}$ ), an inhibitor of enzymatic  $\text{H}_2\text{S}$  synthesis,<sup>2b</sup> to show the reduced green fluorescence from L-Cys-treated cells (Fig. 5b). These results suggest that D-Cys should be mainly metabolized into  $\text{H}_2\text{S}$ , whereas L-Cys could be expressed as both  $\text{H}_2\text{S}$  and GSH (Fig. 5c), resulting in dual activations of the probe.

## Conclusions

In summary, we rationally designed and synthesized the first dual-reactive fluorescent probe based on NBD amine and CBD arylether for dual-activated detection from  $\text{H}_2\text{S}$  + GSH, which is also the first example of the combination between CBD arylether and another sensing motif. Probe **1** shows very weak background fluorescence due to the dual-quenching effects, and can be dual-activated by the co-existence of  $\text{H}_2\text{S}$  and GSH

with a 500-fold fluorescence increase at 525 nm. Moreover, probe **1** exhibits high sensitivity, excellent selectivity, and good biocompatibility, all of which enable us to detect the intracellular  $\text{H}_2\text{S}$  and GSH. Based on this probe tool, we demonstrate the biogenesis of both  $\text{H}_2\text{S}$  and GSH from L-Cys rather than from D-Cys in live cells. These metabolic differences of chiral Cys help understand that the treatment of D-Cys has been shown to elevate the  $\text{H}_2\text{S}$  level more effectively than L-Cys in live cells.<sup>17</sup> Moreover, we believe that such multi-reactive multi-quenching probes are useful for investigating the crosstalk and relationship of other biological molecules in the future.

## Conflicts of interest

There are no conflicts to declare.

## Acknowledgements

We thank Prof. Zhen Xi at Nankai University for kind support. We acknowledge the support of NSFC (22177010).

## Notes and references

- (a) G. Yang, L. Wu, B. Jiang, W. Yang, J. Qi, K. Cao, Q. Meng, A. K. Mustafa, W. Mu, S. Zhang, S. H. Snyder and R. Wang, *Science*, 2008, **332**, 587; (b) X. Cao, L. Ding, Z. Xie, Y. Yang, M. Whiteman, P. K. Moore and J.-S. Bian, *Antioxid. Redox Signaling*, 2019, **31**, 1–38; (c) M. R. Filipovic, J. Zivanovic, B. Alvarez and R. Banerjee, *Chem. Rev.*, 2018, **118**, 1253–1337; (d) M. Trujillo, B. Alvarez and R. Radi, *Free Radical Res.*, 2016, **50**, 150–171; (e) F. Rabe von Pappenheim, M. Wensien, J. Ye, J. Uranga, I. Irisarri, J. de Vries, L.-M. Funk, R. A. Mata and K. Tittmann, *Nat. Chem. Biol.*, 2022, **18**, 368–375; (f) P. Bora, S. Manna, M. A. Nair, R. R.-M. Sathe, S. Singh, V. S. Sreyas Adury, K. Gupta, A. Mukherjee, D. K. Saini, S. S. Kamat, A. B. Hazra and H. Chakrapani, *Chem. Sci.*, 2021, **12**, 12939–12949; (g) C. M. Levinn, M. M. Cerda and M. D. Pluth, *Acc. Chem. Res.*, 2019, **52**, 2723–2731; (h) X. Ni, S. S. Kelly, S. Xu and M. Xian, *Acc. Chem. Res.*, 2021, **54**, 3968–3978.
- (a) R. Wang, *Physiol. Rev.*, 2012, **92**, 791–896; (b) C. Szabo, *Biochem. Pharmacol.*, 2018, **149**, 5–19; (c) Y. Liu, M. Lu, L. Hu, P. T. Wong, G. D. Webb and J. Bian, *Antioxid. Redox Signaling*, 2012, **17**, 141–185; (d) K. Modis, Y. Ju, A. Ahmad, A. A. Untereiner, Z. Altaany, L. Wu, C. Szabo and R. Wang, *Pharmacol. Res.*, 2016, **113**, 116–124; (e) V. S. Khodade, S. C. Aggarwal, B. M. Pharoah, N. Paolucci and J. P. Toscano, *Chem. Sci.*, 2021, **12**, 8252–8259.
- (a) K. Yang, F. Cao, L. Tao, Y. Zhu and Y. Xue, *Front. Physiol.*, 2022, **13**, 840293; (b) T. Liu, L. Sun, Y. Zhang, Y. Wang and J. Zheng, *J. Biochem. Mol. Toxicol.*, 2022, **36**, e22942; (c) R. A. Cairns, I. S. Harris and T. W. Mak, *Nat. Rev. Cancer*, 2011, **11**, 85–95; (d) C. Hwang, A. J. Sinskey and H. F. Lodish, *Science*, 1992, **257**, 1496–1502.
- (a) H. Kimura, *Amino Acids*, 2011, **41**, 113; (b) N. Shibuya, S. Koike, M. Tanaka, M. Ishigami-Yuasa, Y. Kimura, Y. Ogasawara,



- K. Fukui, N. Nagahara and H. Kimura, *Nat. Commun.*, 2013, **4**, 1366; (c) B. D. Paul, J. I. Sbodio and S. H. Snyder, *Trends Pharmacol. Sci.*, 2018, **39**, 513–524; (d) S. C. Lu, *Biochim. Biophys. Acta, Gen. Subj.*, 2013, **1830**, 3143–3153; (e) M. H. Stipanuk, *Annu. Rev. Nutr.*, 2004, **24**, 539–577.
- 5 (a) C. Szabo, *Nat. Rev. Drug Discovery*, 2016, **15**, 185–203; (b) C. Szabo and A. Papapetropoulos, *Pharmacol. Rev.*, 2017, **69**, 497–564; (c) J. Dorszewska, M. Prendecki, A. Oczkowska, M. Dezor and W. Kozubski, *Curr. Alzheimer Res.*, 2016, **13**, 952–963; (d) L. Kennedy, J. K. Sandhu, M. Harper and M. Cuperlovic-Culf, *Biomolecules*, 2020, **10**, 1429; (e) C. Coletta, K. Modis, B. Szczesny, A. Brunyanszki, G. Olah, E. C.-S. Rios, K. Yanagi, A. Ahmad, A. Papapetropoulos and C. Szabo, *Mol. Med.*, 2015, **21**, 1–14.
- 6 (a) S. Seshadri, A. Beiser, J. Selhub, P. F. Jacques, I. H. Rosenberg, R. B. D'Agostino, P. W. Wilson and P. A. Wolf, *N. Engl. J. Med.*, 2002, **346**, 476–483; (b) Y. Chen, H. Dong, D. C. Thompson, H. G. Shertzer, D. W. Nebert and V. Vasiliou, *Food Chem. Toxicol.*, 2013, **60**, 38–44; (c) Y. Xiong, C. Xiao, Z. Li and X. Yang, *Chem. Soc. Rev.*, 2021, **50**, 6013–6041; (d) O. Karmin and Y. L. Siow, *Curr. Med. Chem.*, 2018, **25**, 367–377.
- 7 W.-N. Niu, P. K. Yadav, J. Adamec and R. Banerjee, *Antioxid. Redox Signaling*, 2015, **22**, 350–361.
- 8 (a) X. Chen, Y. Zhou, X. Peng and J. Yoon, *Chem. Soc. Rev.*, 2010, **39**, 2120–2135; (b) L.-Y. Niu, Y.-Z. Chen, H.-R. Zheng, L.-Z. Wu, C.-H. Tung and Q.-Z. Yang, *Chem. Soc. Rev.*, 2015, **44**, 6143–6160; (c) V. S. Lin, W. Chen, M. Xian and C. J. Chang, *Chem. Soc. Rev.*, 2015, **44**, 4596–4618; (d) Y. Yue, F. Huo and C. Yin, *Chem. Sci.*, 2021, **12**, 1220–1226; (e) Z. Xu, X. Huang, X. Han, D. Wu, B. Zhang, Y. Tan, M. Cao, S.-H. Liu, J. Yin and J. Yoon, *Chem.*, 2018, **4**, 1609–1628; (f) I. Ismail, Z. Chen, L. Sun, X. Ji, H. Ye, X. Kang, H. Huang, H. Song, S. G. Bolton, Z. Xi, M. D. Pluth and L. Yi, *Chem. Sci.*, 2020, **11**, 7823–7828; (g) H. Z. Liu, W. T. Song, S. R. Zhang, K. S. Chan, Z. J. Guo and Z. Shen, *Chem. Sci.*, 2020, **11**, 8495–8501; (h) X. Tian, L. C. Murfin, L. Wu, S. E. Lewis and T. D. James, *Chem. Sci.*, 2021, **12**, 3406–3426; (i) R. Zhang, J. Yong, J. Yuan and Z. P. Xu, *Coord. Chem. Rev.*, 2020, **408**, 213182; (j) Z. Liu, W. Zhou, J. Li, H. Zhang, X. Dai, Y. Liu and Y. Liu, *Chem. Sci.*, 2020, **11**, 4791–4800; (k) M. Yang, J. Fan, J. Du and X. Peng, *Chem. Sci.*, 2020, **11**, 5127–5141; (l) X. Wang, J. Zha, W. Zhang, W. Zhang and B. Tang, *Analyst*, 2020, **145**, 6119–6124; (m) M. D. Pluth, Y. Zhao and M. M. Cerda, *Methods Enzymol.*, 2020, **641**, 149–164; (n) A. P.-A. Dos Santos, J. K. da Silva, J. M. Neri, A. C.-O. Neves, D. F. de Lima and F. G. Menezes, *Org. Biomol. Chem.*, 2020, **18**, 9398–9427; (o) C. Jiang, H. Huang, X. Kang, L. Yang, Z. Xi, H. Sun, M. D. Pluth and L. Yi, *Chem. Soc. Rev.*, 2021, **50**, 7436–7495; (p) J. M. An, S. Kang, E. Huh, Y. Kim, D. Lee, H. Jo, J. F. Joung, V. J. Kim, J. Y. Lee, Y. S. Dho, Y. Jung, J. K. Hur, C. Park, J. Jung, Y. Huh, J.-L. Ku, S. Kim, T. Chowdhury, S. Park, J. S. Kang, M. S. Oh, C.-K. Park and D. Kim, *Chem. Sci.*, 2020, **11**, 5658–5668; (q) H. Zong, J. Peng, X.-R. Li, M. Liu, Y. Hu, J. Li, Y. Zang, X. Li and T. D. James, *Chem. Commun.*, 2020, **56**, 515–518; (r) Y. Zou, M. Li, Y. Xin, T. Duan, X. Zhou and F. Yu, *ACS Sens.*, 2020, **5**, 242–249; (s) X. Zhang, W. Qu, H. Liu, Y. Ma, L. Wang, Q. Sun and F. Yu, *Anal. Chim. Acta*, 2020, **1109**, 37–43.
- 9 (a) J. Liu, Y.-Q. Sun, Y. Huo, H. Zhang, L. Wang, P. Zhang, D. Song, Y. Shi and W. Guo, *J. Am. Chem. Soc.*, 2014, **136**, 574–577; (b) H. Zhang, R. Liu, J. Liu, L. Li, P. Wang, S. Q. Yao, Z. Xu and H. Sun, *Chem. Sci.*, 2016, **7**, 256–260; (c) C.-X. Yin, K.-M. Xiong, F.-J. Huo, J. C. Salamanca and R. M. Strongin, *Angew. Chem., Int. Ed.*, 2017, **56**, 13188–13198; (d) Z. Xu, T. Qin, X. Zhou, L. Wang and B. Liu, *Trends Anal. Chem.*, 2019, **121**, 115672; (e) D. Qiao, T. Shen, M. Zhu, X. Liang, L. Zhang, Z. Yin, B. Wang and L. Shang, *Chem. Commun.*, 2018, **54**, 13252–13255; (f) J. Li, C. Yin, Y. Zhang, Y. Yue, J. Chao and F. Huo, *Dyes Pigm.*, 2020, **172**, 107826; (g) Z. Chai, Q. Wu, K. Cheng, X. Liu, L. Jiang, M. Liu and C. Li, *Chem. Sci.*, 2021, **12**, 1095–1100; (h) H. Huang, X. Ji, Y. Jiang, C. Zhang, X. Kang, J. Zhu, L. Sun and L. Yi, *Org. Biomol. Chem.*, 2020, **18**, 4004–4008; (i) J. Liu, M. Liu, H. Zhang, X. Wei, J. Wang, M. Xian and W. Guo, *Chem. Sci.*, 2019, **10**, 10065–10071; (j) J. Zhang, Y. Zhang, Q. Guo, G. Wen, H. Xiao, S. Qi, Y. Wang, H. Zhang, L. Wang and H. Sun, *ACS Sens.*, 2022, **7**, 1105–1112.
- 10 (a) H. Zhang, C. Zhang, R. Liu, L. Yi and H. Sun, *Chem. Commun.*, 2015, **51**, 2029–2032; (b) C. Zhang, L. Wei, C. Wei, J. Zhang, R. Wang, Z. Xi and L. Yi, *Chem. Commun.*, 2015, **51**, 7505–7508; (c) G. Zheng, Z. Li, Q. Duan, K. Cheng, Y. He, S. Huang, H. Zhang, Y. Jiang, Y. Jia and H. Sun, *Sens. Actuators, B*, 2020, **310**, 127890; (d) H. Tong, J. Zhao, X. Li, Y. Zhang, S. Ma, K. Lou and W. Wang, *Chem. Commun.*, 2017, **53**, 3583–3586; (e) F.-F. Wang, Y.-J. Liu, B.-B. Wang, L.-X. Gao, F.-L. Jiang and Y. Liu, *Dyes Pigm.*, 2018, **152**, 29–35; (f) B.-J. Wang, R.-J. Liu, J. Fang, Y.-W. Wang and Y. Peng, *Chem. Commun.*, 2019, **55**, 11762–11765; (g) Y. Jiang, G. Zheng, Q. Duan, L. Yang, J. Zhang, H. Zhang, J. He, H. Sun and D. Ho, *Chem. Commun.*, 2018, **54**, 7967–7970.
- 11 C. Zhang, R. Wang, L. Cheng, B. Li, Z. Xi and L. Yi, *Sci. Rep.*, 2016, **6**, 30148.
- 12 (a) C. Zhang, Q.-Z. Zhang, K. Zhang, L.-Y. Li, M. D. Pluth, L. Yi and Z. Xi, *Chem. Sci.*, 2019, **10**, 1945–1952; (b) C. Liu, R. Zhang, W. Zhang, J. Liu, Y. L. Wang, Z. Du, B. Song, Z. P. Xu and J. Yuan, *J. Am. Chem. Soc.*, 2019, **141**, 8462–8472; (c) C. Du, S. Fu, X. Wang, A. C. Sedgwick, W. Zhen, M. Li, X. Li, J. Zhou, Z. Wang, H. Wang and J. L. Sessler, *Chem. Sci.*, 2019, **10**, 5699–5704; (d) J. Xie, R. Mu, M. Fang, Y. Cheng, F. Senchyna, A. Moreno, N. Banaeibcd and J. Rao, *Chem. Sci.*, 2021, **12**, 9153–9161.
- 13 X. Tu, L. He, H. Huang, H. Ye, L. Sun and L. Yi, *Chem. Commun.*, 2021, **57**, 8802–8805.
- 14 (a) R. Wang, Z. Li, C. Zhang, Y. Li, G. Xu, Q.-Z. Zhang, L.-Y. Li, L. Yi and Z. Xi, *ChemBioChem*, 2016, **17**, 962–968; (b) R. Chen, H. Ye, T. Fang, S. Liu, L. Yi and L. Cheng, *Org. Biomol. Chem.*, 2022, **20**, DOI: [10.1039/D2OB00442A](https://doi.org/10.1039/D2OB00442A).
- 15 Y. Zhao, A. K. Steiger and M. D. Pluth, *J. Am. Chem. Soc.*, 2019, **141**, 13610–13618.
- 16 (a) X. Jiang, Y. Yu, J. Chen, M. Zhao, H. Chen, X. Song, A. J. Matzuk, S. L. Carroll, X. Tan, A. Sizovs, N. Cheng, M. Wang and J. Wang, *ACS Chem. Biol.*, 2015, **10**, 864–874; (b) Z. Liu, X. Zhou, Y. Miao, Y. Hu, N. Kwon, X. Wu and J. Yoon, *Angew. Chem., Int. Ed.*, 2017, **56**, 5812–5816.
- 17 (a) L. Wei, L. Yi, F. B. Song, C. Wei, B. F. Wang and Z. Xi, *Sci. Rep.*, 2014, **4**, 4521; (b) L. Wei, Z. Zhu, Y. Li, L. Yi and Z. Xi, *Chem. Commun.*, 2015, **51**, 10463–10466.

